Magnetic properties of the Fe-MgO interface studied by Mössbauer spectroscopy

J. Balogh,[1,*] I. Dézsi,[1] Cs. Fetzer,[1] J. Korecki,[2,3] A. Kozioł-Rachwał,[2] E. Młyńczak,[3] and A. Nakanishi[4]
[1]*Wigner Research Centre for Physics, Hungarian Academy of Sciences H-1525 Budapest 114 P.O. Box 49, Hungary*
[2]*Faculty of Physics and Applied Computer Science, AGH University of Science and Technology, 30-059 Krakow, Poland*
[3]*Jerzy Haber Institute of Catalysis and Surface Chemistry, Polish Academy of Sciences, 30-239 Krakow, Poland*
[4]*Department of Physics, Shiga University of Medical Science, Shiga 520-2192, Japan*
(Received 9 January 2013; revised manuscript received 26 April 2013; published 9 May 2013)

Thin ^{57}Fe layers evaporated onto an MgO(100) single-crystal substrate and covered by an evaporated MgO layer were studied by low-temperature conversion electron Mössbauer spectroscopy. The temperature dependence of the spectra indicates superparamagnetic behavior below 8 ML nominal thickness of the Fe layer signaling a cluster-type growth mode. The low-temperature hyperfine fields are consistent with a model that defines two types of metallic Fe atoms: bulklike and interfacial ones. Formation of FeO or (Fe,Mg)O at the interface layer is not observed. The sample with a 4-ML Fe layer when grown over a cleaved MgO substrate shows almost perfect perpendicular magnetization, as locally probed at 15 K by the hyperfine magnetic field, while random magnetization orientation and lower blocking temperature is observed in the case of a polished substrate. The perpendicular anisotropy observed at low temperature is attributed to mechanical stresses arising from the epitaxial relation and the different temperature dilatation of the subsequent layers.

DOI: 10.1103/PhysRevB.87.174415 PACS number(s): 76.80.+y, 68.35.−p, 75.70.Cn

I. INTRODUCTION

The structural, electronic, and magnetic properties of the Fe-MgO interface have attracted a lot of interest for a long time. MgO single crystals have been frequently used as substrate material to Fe thin films because of the attainable epitaxial growth mode with a small lattice mismatch.[1–3] The theoretically predicted[4] lack of electronic interaction between Fe and MgO and the calculated giant Fe monolayer magnetization inspired many experimental works on the magnetic properties of Fe thin films over MgO substrates.[5–11] Also a large number of works has been devoted to Fe/MgO multilayered structures.[12–16] In agreement with an early paper,[4] recent *ab initio* spin-density-functional calculations[17] indicated an increased magnetic moment ($2.94\mu_B$) at the (001) surface of the bcc-Fe layer and pointed to the role of in-plane tensile strains in a further increase of it. Next, the prediction of a very high tunneling magnetoresistance of Fe/MgO/Fe trilayers[18,19] can be pointed to in the row of theoretical works that had a significant impact on the experimental studies.[20] At present, the Fe-MgO system is considered as part of the heterostuctures[21,22] constructed to utilize the magnetoelectric effect,[23,24] which arises from the spin-dependent screening of the electric field at the surface or interface of a ferromagnetic metal.

The preparation-dependent structural[25,26] and chemical properties of the metal-insulator interface have a key role in the actual value of the Fe magnetic moment, the magnetic anisotropy, or the tunneling magnetoresistance. The formation of FeO at the interface has been proposed in many works,[27–32] but there are a number of experimental reports on the absence of it[33–37] as well. While the experimental results are controversial, theoretical calculations on the magnetic and transport properties attribute a significant effect to the structural and oxidation state at the interface.[38,39]

Mössbauer spectroscopy is one of the most sensitive methods to investigate the charge state and the magnetic moment of the interfacial Fe atoms. In the literature, however, there are relatively few studies of the Fe-MgO interface.[8,12,40,41] To study a few monolayers of Fe, conversion electron Mössbauer spectroscopy (CEMS) is the most effective method, since 90% of the utilized nuclear deexcitations takes place not by γ radiation, but through the emission of conversion electrons. In spite of this, the first studies[12,40] were made on evaporated MgO and Fe layers over different substrate materials to facilitate absorption measurements, which are more easy to carry out at low temperatures. Thin Fe layers epitaxially grown over MgO single crystal substrates have only been measured above 80 K by CEMS.[8] A CEMS measurement performed at 4.2 K can be found in the case of a multicomponent heterostructure[42] containing a 5-monolayers (ML) ^{57}Fe layer, which is grown over a 3-nm evaporated MgO(001) layer and capped by a Fe-Tb multilayer structure and Cr.

Low-temperature measurements are essential to study the interface properties since few-ML-thick Fe layers were reported to be superparamagnetic at elevated temperatures in many studies,[5,8,10,13–15,26,43] indicating a discontinuous layer over the MgO substrate. Beyond possible experimental errors, superparamagnetic relaxation and oxide formation can both play a role in the controversial experimental results[44,45] on the value of the Fe magnetic moment at the interface. While the formation of a ∼2–3-Å thick magnetically dead layer[44] was attributed to chemical intermixing and a consequent FeO formation at the Fe/MgO interface, the observation of a $4\mu_B$ magnetic moment at small Fe thickness[45] was also explained by a charge transfer between the facing O and Fe atoms.

The aim of the present work is to study by Mössbauer spectroscopy the extent of charge transfer and magnetic moment perturbation at the Fe-MgO interface. This will be examined in the case of few-ML-thick Fe layers grown epitaxially over single crystal MgO(100) substrates and caped by a vacuum evaporated MgO layer. The effect of substrate treatment, e.g., cleaving or polishing, will also be studied, since it was shown previously that the form of MgO substrates plays an important role on the structural and magnetic properties

of iron films.[8] To rule out the effect of superparamagnetic relaxations, former studies[8,41] will be complemented by CEMS measurements at 15 K.

II. EXPERIMENTAL

The samples were prepared and characterized in a multichamber UHV system[46] with the base pressure below 10^{-10} mbar. The system was equipped with a load-lock facility, a universal sample mounting and transfer system, standard surface characterization methods [a four-greed electron optics for low-energy electron diffraction (LEED) and Auger electron spectroscopy], an MBE system for deposition of several metals including ^{57}Fe isotopes, and a CEMS spectrometer. All samples were deposited on MgO(001) substrates that were cleaved *ex situ* prior to the introduction into the UHV system or on polished ones. The substrates were UHV annealed at 990 K for 30 min. For the cleaved substrates, such treatment resulted in a clean surface showing only traces of carbon contamination and a perfect background-free 1×1 LEED pattern. The cleanness of the polished substrate was further improved by depositing a thin (around 50 Å) homoepitaxial MgO layer on the substrate kept at 990 K.

Iron, enriched to 90% with the ^{57}Fe isotope, was deposited from a BeO crucible heated by wraparound tungsten coils. The crucible assemblies were embedded in a water-cooled shroud and the pressure during the deposition remained in the 10^{-10} mbar range. The series of samples containing 4, 6, 8, and 10 ML ^{57}Fe layer were grown at a rate of 0.025 ML/s. The MgO buffer and capping layers were evaporated by electron bombardment from a single crystal piece. The film thickness was controlled during the deposition by quartz thickness monitors with an accuracy of about 0.2 ML. The Fe and the capping layers were deposited on substrates kept at room temperature.

The Fe films were characterized *in situ*[8] by LEED. The LEED patterns showed an epitaxial growth of (001) oriented films with in-plane crystallographic relations: Fe[100]||MgO[110]. Broadened LEED spots indicated imperfect growth: nucleation of small islands resulted in granular film structures. There was no apparent difference in the LEED patterns for the films grown on cleaved and polished substrates.

The Mössbauer measurements were carried out by using a conventional constant acceleration-type spectrometer. For the detection of the conversion electrons, a low-background proportional counter filled with H_2 was used at low temperatures.[47] At temperatures higher than 70 K, a 96%He-4%CH_4 gas mixture was used for the measurement. The spectra were measured by a 50 mCi ^{57} Co(Rh) single line source. The isomer shift (IS) values are given relative to that of α-Fe at room temperature.

III. EXPERIMENTAL RESULTS

The room-temperature spectra of the samples show pronounced differences, as it can be seen in Fig. 1. While relaxation broadening of the lines and the appearance of paramagnetic components are observed in the case of the 4- and 6-ML samples, the 8- and 10-ML samples show magnetically split spectra that can be described by two modestly broadened

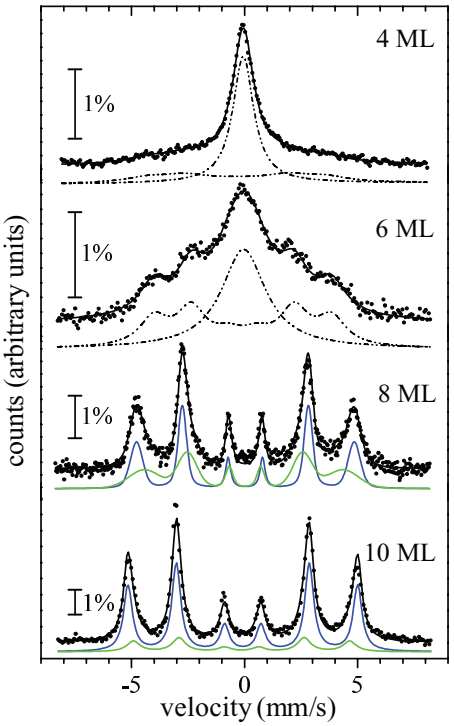

FIG. 1. (Color online) Room-temperature CEMS of samples over cleaved MgO(100) substrate with ^{57}Fe layer thickness as indicated in the figure. The fitted subspectra (see text for details) are also indicated. The scale bars indicate the 1% relative transmission.

sextets. The linewidth is close to 0.6 mm/s for the 10-ML sample while a Voight line profile[48] with 1.4 and 3.7-T width for the two components could be fitted to the spectrum of the 8-ML sample. The hyperfine fields (HF-s) are significantly lower than the 33 T value of bulk bcc-Fe even for the larger field components (29.9 and 31.5 T for the 8- and 10-ML samples, respectively). The evaluation of the spectra of the 4- and 6-ML samples by components with Lorentzian line shape, as shown in Fig. 2, is evidently not physically meaningful, however, it is often used[49] in order to make an approximation on the superparamagnetic blocking temperature. The superparamagnetic relaxation emerges as a broadening of the lines and a change of the line shape of the magnetic sextets at low frequencies, which gradually collapse into a single line at higher frequencies. Size distribution of the grains always results in the coexistence of magnetically split and single line components over a certain temperature range. Experimentally, the blocking temperature can be defined as the temperature where the paramagnetic and magnetic components have equal spectral fraction. This way, the blocking temperature of the 4-ML sample is lower than that of the 6-ML sample. The broad lines and the low values of the hyperfine field as compared to the bulk one in case of the 8- and 10-ML samples might also be due to a slow relaxation as a consequence of blocking temperature above room temperature.

The low-temperature CEMS spectra of the sample series on cleaved substrates are shown in Fig. 2. At 15 K, all the samples show magnetic splitting with no appreciable paramagnetic line. (A very small paramagnetic component is present in the 4-ML sample.) The width of the lines is significantly broader

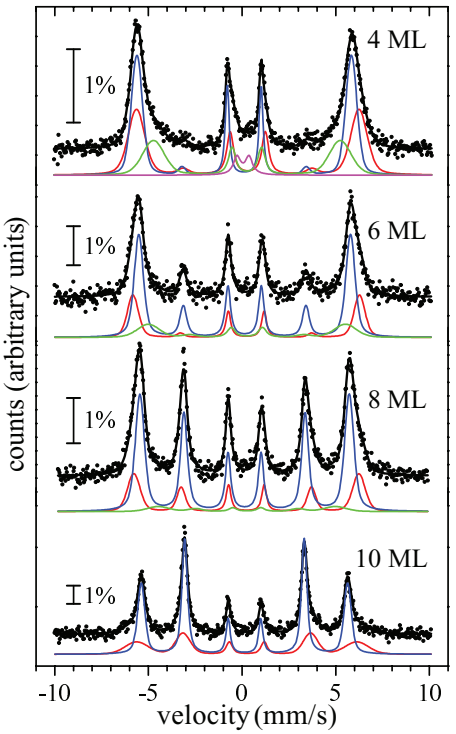

FIG. 2. (Color online) Conversion electron Mössbauer spectra of the samples over cleaved MgO(100) substrates with different ^{57}Fe layer thickness as measured at 15 K. The calculated spectra result from fitting by sextets—indicated by the subspectra for each spectrum—which have lines with Voight line shape. In case of the 4-ML sample, a small quadruple doublet is also present among the components. The scale bars indicate a 1% relative transmission.

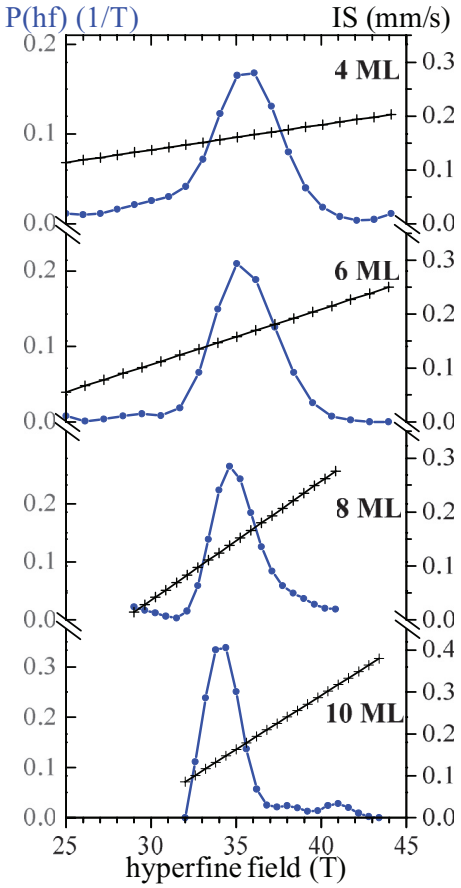

FIG. 3. (Color online) Hyperfine field distributions [connected (blue) dots] and the isomer shift values [connected (black) crosses] linearly correlated to the hyperfine fields. The spectral intensity of the components is shown on the left scale and the isomer shifts on the right scale.

than the experimental linewidth (0.25 mm/s) indicating a distribution of the hyperfine parameters. The hyperfine field distributions evaluated by the Hesse-Rübartsch method,[50] i.e., by a set of 20 subsextets in the range of 25 to 45 T with linewidth fixed to 0.3 mm/s, are shown in Fig. 3 and the calculated average parameters are summarized in Table I. The IS is supposed to be linearly correlated with the hyperfine field in the calculations, the fitted linear functions are also plotted in Fig. 3. A uniform quadrupole splitting (QS) of the subsextets was also allowed, but the fitted values were close to zero.

Since the above calculations contain a restriction on the IS distribution, the low-temperature spectra were also evaluated by independent sextets with Voight line broadening. Three independent components resulted in χ^2 values comparable to those obtained by the Hesse-Rübartsch method in case of the 4-, 6-, and 8-ML samples, while for the 10-ML sample two components were enough to produce a similar quality fit. The parameters of these evaluations are summarized in Table II, while Fig. 2 shows the calculated spectra for the Voight-type evaluation and the fitted subspectra for each sample.

TABLE I. Calculated values belonging to the distributions shown in Fig. 3. HF_{av} and IS_{av} are the average values of the hyperfine field and the isomer shift, STD is the standard deviation of the Hf distribution, >36T stands for the sum of the spectral intensity of the subsextets above 36 T, and I_{2-5} is the fitted common relative amplitude of the 2nd and 5th lines of the subsextets.

ML	HF_{av} (T)	STD(T)	>36T (%)	IS_{av} (mm/s)	I_{2-5}
4	35.02(7)	3.26(8)	47	0.161(1)	0.15(2)
6	35.49(13)	2.72(18)	47	0.163(10)	0.56(3)
8	35.20(4)	2.05(5)	26	0.151(1)	1.86(3)
10	34.83(5)	1.98(9)	15	0.159(1)	3.89(6)

The two kinds of evaluations—histogram-type distribution and three or two independent components broadened by a Voight profile—resulted in similar average values of the hyperfine field, and the I_{2-5} amplitudes as can be seen comparing Tables I and II.

Both types of evaluation indicate a significant fraction of Fe atoms that have HFs much larger than that of bulk bcc-Fe at low temperature (33.8 T). The component around 37 T in the Voight-profile fit has intensities around 30% for all the samples. For comparison, the sum of the normalized probabilities above 36 T in case of the hyperfine field distributions of Fig. 2 is also shown in Table I. These numbers also indicate a large number of Fe atoms with an increased hyperfine field in all the samples. Here, we note that in case of the thinner samples the intensity of these components decreases smoothly with increasing hyperfine field. The small peaks around 41 and 38 T in case of the 10-ML Fe sample

TABLE II. Hyperfine fields (HF1, HF2, and HF3) and spectral ratios (A1, A2, A3) of the fitted components shown in Fig. 2. HF_{av}, IS_{av}, and I_{2-5} are the average values of the hyperfine field, the isomer shift, and the relative amplitude of the 2nd and 5th lines of the components.

ML	HF1 (T)	HF2 (T)	HF3 (T)	A1 (%)	A2 (%)	A3 (%)	HF_{av} (T)	IS_{av} (mm/s)	I_{2-5}
4	36.8(3)	35.5(1)	30.9(10)	34(8)	40(6)	22(7)	34.9	0.21(3)	0.1(1)
6	37.5(4)	35.0(1)	32.6(13)	25(6)	60(9)	15(6)	35.3	0.18(5)	0.6(2)
8	37.3(3)	34.7(1)	29.4(10)	25(4)	69(4)	7(1)	35.0	0.16(1)	1.8(1)
10	36.5(4)	34.2(1)	...	31(4)	69(4)	...	34.9	0.17(2)	3.8(2)

are typical artifacts of the fitting procedure.[51] If they were connected to some interface property, they would show up even more intensively for the thinner Fe layers, which is not the case. The contribution of the low-field components around 30 T is smaller and decreases fast with the increase of the Fe layer thickness. As an interplay of the gradual decrease of the hyperfine field of the central component and the decreasing intensity of the low-field components, the average hyperfine field remains constant within the experimental errors. The IS values of the independent sextets (not shown in the table) slightly deviate from the value corresponding to the respective value of HF in Fig. 3, being in the 0.22–0.3 mm/s range both for the low- and the high-field components, which explains the slightly larger average IS values, as compared to those in Table I.

The most conspicuous difference among the spectra of Fig. 2 lies in the gradual increase of the intensity of the 2nd and 5th lines (I_{2-5}) as the Fe layer thickness increases. Note that I_{2-5} was supposed to be equal for all the 20 subsextets of the distributions, while it was an independent parameter for the components in the Voight-type evaluations. In the latter case, the I_{2-5} values were systematically slightly smaller for the high-field components (0.2, 1.4, and 3.4 for the 6-, 8-, and 10-ML samples, respectively) than that of the central one (0.7, 2.0, and 4.0 for the 6-, 8-, and 10-ML samples, respectively). The I_{2-5} line intensities give information on the direction of the average magnetization according to the formula $I_{2-5} = 4\sin^2\theta \,/\, (1+\cos^2\theta)$, where θ is the angle between the direction of the magnetization and the γ rays. According to this, the spontaneous magnetization of the 4-ML sample is almost parallel to the γ rays, i.e., perpendicular to the sample plane at 15 K. The 10-ML sample shows an in-plane magnetization both at room and low temperatures, while in case of the 8-ML sample the magnetization changes direction with temperature, as it can be seen by comparing the respective spectra of Figs. 1 and 2. This behavior was further studied at intermediate temperatures and a continuous change of I_{2-5} is observed, as it is shown in Fig. 4.

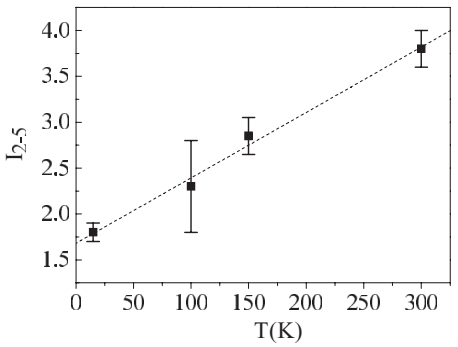

FIG. 4. Temperature dependence of the intensities of the lines belonging to the $\Delta m = 0$ transitions in case of the 8-ML sample.

The spectra of 4 ML ^{57}Fe grown on a polished MgO substrate and measured at 15 and 300 K are shown in Fig. 5. The room-temperature spectrum can be described with a singlet (IS = 0.05 mm/s) and a doublet (IS = 0.2 mm/s, QS = 0.74 mm/s), similarly to that what was observed earlier[8] for a 5-ML sample. The presence of fast relaxing components is evident even at 15 K and the magnetically split component is broader and has a smaller average HF (33 T) than in case of the 4-ML sample over cleaved MgO. The I_{2-5} value is also very different ($I_{2-5} \approx 2$), which is probably due to a random distribution of the magnetization directions. All these features can be due to a blocking temperature close to 15 K.

IV. DISCUSSION

The evaluated HFs and ISs indicate metallic Fe layers over the MgO substrate in all the samples. Charge transfer between the Fe and O atoms, i.e., the formation of significant amount of $Fe_{1-x}O$ (wüstit) or (Mg,Fe)O (mineral name ferropericlase) is

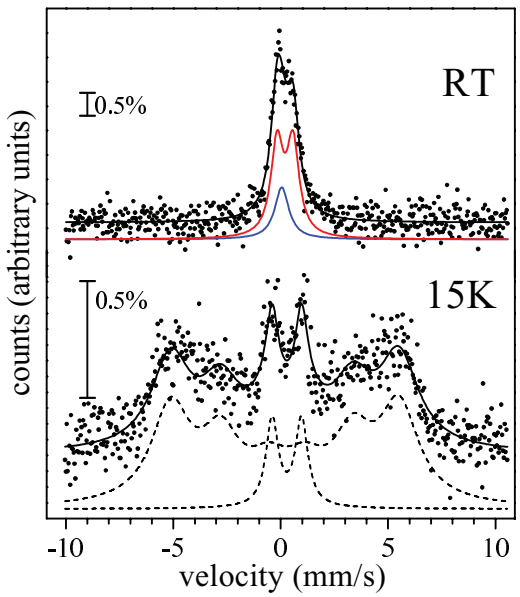

FIG. 5. (Color online) CEMS of a 4-ML thick ^{57}Fe layer grown over a polished MgO(100) substrate and covered by an evaporated MgO layer as measured at the indicated temperatures. For the indicated components see text. The scale bars indicate the 0.5% relative transmission.

not supported by our Mössbauer measurements. The hyperfine parameters of these compounds have been studied extensively since long as they depend on stoichiometry and defect structure. Bulk wüstit is paramagnetic at room temperature and—except the case when x is close to zero—the spectrum shows an apparent quadrupole doublet with broad lines which can be decomposed into sub-sub-spectra belonging to Fe^{2+} and Fe^{3+}atoms at different lattice sites.[52,53] The largest contribution comes from Fe^{2+} ions at regular octahedral sites that give quadrupole splitting around 0.6 mm/s and IS around 1 mm/s. Below about 195 K, wüstit orders antiferromagnetically and the 4.2 K spectrum consists of magnetically split components in the range of 38–51 T. Ferropericlase is paramagnetic even at 80 K and also shows large IS and QS in the whole solid solution range.[54] The CEMS of FeO ultrathin films on MgO substrate have also been studied[55] and beyond the close-to-bulk components, a FeO-MgO interface component was identified with IS and QS approaching 0.9 and 2 mm/s, respectively. When comparing all these results to the parameters of Tables I and II, we can safely exclude the presence of a significant amount of $Fe_{1-x}O$ or (Mg,Fe)O. For example, in case of the 4-ML sample, if we add further components to those listed in Table II and fix their hyperfine parameters to the value typical for Fe^{2+} in wüstit, the fitting allows less than 5% spectral area for these components. This means less than 0.2-ML Fe atoms at the two interfaces, i.e., 0.1 ML as an upper limit for the amount of Fe atoms in chemical interaction with the neighboring oxygen atoms at the interface. Further studies of samples with thinner Fe layers or transmission measurements of multilayers in external field might allow a more precise determination of this number.

Comparison of the spectra measured at 300 and 15 K (see Figs. 1 and 2) makes it evident that the variation of the 300 K spectra with increasing Fe layer thickness, and the appearance of broad magnetically split components indicate the presence of superparamagnetic relaxation for samples below 8-ML Fe thickness. This finding is consistent with the Fe percolation threshold around 0.8 nm, which was deduced from different magnetic measurements.[13,14,43] The few-ML percolation threshold is a consequence of the cluster-type growth mode, and below this limit, the increasing superparamagnetic blocking temperature signals the increasing average cluster size.

The three components fitted to the 15-K spectra belong to Fe atoms in different local neighbourhoods. The HFs of the second components agree well with the position of the maximum of the distributions in Fig. 3 and they lay closest to those of bcc Fe. The intensity of this component increases with increasing Fe layer thickness and can be attributed to Fe atoms in the center of the Fe layer. The IS values also support this assignment. Dipole fields in the thin layers,[56] as well as lattice strains, may explain the slightly increased HFs as compared to the bulk value.

The origin of the other two components is less straightforward. The relation between the local magnetic moment and the hyperfine field might be similar to other systems where increased magnetic moments and larger than bulk Fe hyperfine fields have been observed, e.g., for Fe-Ag[56,57] and Fe-Pd.[58] Based on theoretical calculations,[58,59] in these systems, the smaller- and larger-than-bulk hyperfine field components were attributed to Fe atoms at the interface and at the subinterface layers, respectively, while the local Fe magnetic moments were larger than the bulk value in both layers. The proportionality (around 15 T/μ_B) generally observed in bulk Fe alloys between the magnetic moment and the hyperfine field is lost at the interface basically due to the valence electron contribution of the contact hyperfine field, which is reduced[59] or changes sign[58] from negative in the interior of the Fe layer to positive at the interface. In case of a perfect layer-by-layer growth, the interface component would make 50%, 33%, 25%, and 20% in case of the 4-, 6-, 8-, and 10-ML thickness, but cluster formation on one hand reduces these numbers and on the other hand broadens the hyperfine field distribution[57] due to the variance in the number of nonmagnetic neighbors at cluster interfaces. The increase of the Fe atomic volume due to the lattice mismatch of the epitaxial layers contributes both to the increase of the magnetic moments and to the appearance of larger-than-bulk hyperfine fields. Here, we note that in case of a special sample structure, MgO/5 ML ^{57}Fe covered by 2.6-nm natural Fe layers and a Fe/Tb multilayer structure, the increased HF is attributed to the dipole field originating from the perpendicular alignment of the magnetization. Our results undoubtedly show that there is a significant amount of increased HF components in case of samples with random or close to in-plane orientation of the magnetization. The volume increase is also in line with the increased IS values, which are, however, not large enough to be explained by the presence of Fe^{2+} ions. Very similar, increased IS values can be observed in various metallic multilayers, e.g., in Fe-Ag.[56,57]

The above interpretations are consistent with that given for the room-temperature paramagnetic spectra,[8] where different ratios of metallic (single line with close to zero IS) and interface (quadrupole doublet) subspectra were decomposed, similarly to what is shown for the present 4-ML sample over the polished substrate in Fig. 5. Both the interface Fe atoms and those in an epitaxially strained lattice can exhibit a quadrupole splitting.

At 15 K, the small value of I_{2-5} in case of the 4-ML sample shows an almost perfect perpendicular alignment of the magnetization, which gradually turns to an in-plane direction as the Fe layer thickness increases. Different magnetic studies have already revealed a variety of anisotropy behaviors of this system[2] as a function of layer thickness and preparation conditions. Beyond the expected in-plane cubic anisotropy, an additional in-plane uniaxial anisotropy[9] was identified in many studies. The appearance of a perpendicular anisotropy component has been observed in Au coated Fe thin layers over MgO substrates.[6] Very large perpendicular anisotropy energies were observed in trilayers of Pt/Co(Fe)/MO_x (M = Ta, Mg, Al, Ru) structures over a silicon wafer,[60,61] which could be achieved by a proper degree of oxidation, and was attributed to the magnetic anisotropy at the Co(Fe)/AlO_x interface. It was associated with the formation of Co-O bonding and the replacement most of the Co-Al bonding at the interface. In recent theoretical calculations[62] concerning the Fe/MgO interface, the perpendicular magnetic anisotropy is ascribed to the hybridization of the Fe-3d and O-2p orbitals, among a few further factors. In our case, an almost perfect perpendicular alignment is realized when a large fraction of close-to-bulk

component is observed and a low upper limit can be set to possible oxide-like components.

The origin of the in-plane to out-of-plain magnetic transition in this system is not yet clear and according to our knowledge neither experimental nor theoretical results on the temperature dependence of the energy of the possible anisotropy components have yet been reported. The variation of I_{2-5} with temperature in case of the 8-ML sample (see Fig. 4) might indicate that strains arising due to different thermal expansion of the layers play a role. An explanation based merely on interface anisotropy is questioned by the cluster-type growth mode and the small (few nm) grain size, which can be deduced from the superparamagnetic behavior. Strain and lattice distortions can very effectively change the magnetic anisotropy and that way epitaxial growth can affect the magnetic state.[63,64] In case of bcc Fe and fcc MgO, the mismatch of the bulk lattice parameters is 4%, but the effective variation may be influenced by lattice relaxation processes and defects. In case of a Fe/MgO multilayer with out of plane magnetization,[65] 1% increase of the Fe lattice parameter was deduced from x-ray line-profile analysis. The variation of the interatomic distances in a 300 K temperature range is an order of magnitude smaller (with bulk parameters) than the above change, however, in case of a delicate balance between anisotropies favoring in-plane and out-of-plane orientations it might play a decisive role. It is interesting to note, however, that a smaller decrease of I_{2-5} was observed in the same temperature range in case of a Fe/Ag multilayer,[66] although the thermal expansion coefficient of Ag ($\approx 19 \times 10^{-6}$ K^{-1}) is larger than that of Fe ($\approx 12 \times 10^{-6}$ K^{-1}) and MgO ($\approx 10 \times 10^{-6}$ K^{-1}). The details of the layer growth can also make a difference as it is demonstrated by the close-to-random distribution of the magnetization in case of the 4-ML sample deposited onto the polished substrate.

V. CONCLUSIONS

We have shown by low-temperature conversion electron Mössbauer spectroscopy measurements of ultrathin Fe layers that charge states of Fe atoms similar to those in $Fe_{1-x}O$ or (Mg,Fe)O are not formed at the Fe-MgO interface. The calculated hyperfine field distributions are comparable to those determined in some metallic multilayers and the hyperfine fields larger than 36 T can be attributed to the interface region between the epitaxial Fe and MgO layers. The observed superparamagnetic behavior is consistent with a cluster-type growth mode. The direction of the spontaneous magnetization changes with the Fe layer thickness and with temperature. At low temperature, an almost perpendicular alignment is observed in case of the smallest nominal Fe layer thickness. The different thermal expansions of the epitaxial layers can play a role in the temperature dependence of the anisotropy directions.

ACKNOWLEDGMENTS

The work was supported by the Hungarian Scientific Research Fund (OTKA) Grant Nos. K 62272 and K 101456. Polish authors acknowledge the financial support of the Polish Ministry of Science and Higher Education and its grants for Scientific Research and of the Foundation for Polish Science.

*balogh.judit@wigner.mta.hu

[1] T. Urano and T. Kanaji, J. Phys. Soc. Jpn. **57**, 3403 (1988).
[2] C. M. Boubeta, J. L. Costa-Krämer, and A. Cebollada, J. Phys.: Condens. Matter **15**, R1123 (2003).
[3] S. Benedetti, P. Myrach, A. di Bona, S. Valeri, N. Nilius, and H. J. Freund, Phys. Rev. B **83**, 125423 (2011).
[4] C. Li and A. J. Freeman, Phys. Rev. B **43**, 780 (1991).
[5] S. Adenwalla, Yongsup Park, G. P. Felcher, and M. Teitelman, J. Appl. Phys. **76**, 6443 (1994).
[6] Y. Y. Huang, C. Liu, and G. P. Felcher, Phys. Rev. B **47**, 183 (1993).
[7] Yu. V. Goryunov, N. N. Garif'yanov, G. G. Khaliullin, I. A. Garifullin, L. R. Tagirov, F. Schreiber, Th. Mühge, and H. Zabel, Phys. Rev. B **52**, 13450 (1995).
[8] M. Zajac, K. Freindl, K. Matlak, M. Slezak, T. Slezak, N. Spiridis, and J. Korecki, Surf. Sci. **601**, 4305 (2007).
[9] Q. Zhan, S. Vandezande, K. Temst, and C. Van Haesendonck, Appl. Phys. Lett. **91**, 122510 (2007).
[10] Seolun Yang, H.-K. Park, J.-S. Kim, J.-Y. Kim, and B.-G. Park, J. Appl. Phys. **110**, 093920 (2011).
[11] S. R. Spurgeon, J. D. Sloppy, R. Tao, R. F. Klie, S. E. Lofland, J. K. Baldwin, A. Misra, and M. L. Taheri, J. Appl. Phys. **112**, 013905 (2012).
[12] T. Koyano, Y. Kuroiwa, E. Kita, N. Saegusa, K. Ohshima, and A. Tasaki, J. Appl. Phys. **64**, 5763 (1988).
[13] A. García-García, A. Vovk, J. A. Pardo, P. Štrichovanec, C. Magén, E. Snoeck, P. A. Algarabel, J. M. De Teresa, L. Morellón, and M. R. Ibarra, J. Appl. Phys. **105**, 063909 (2009).
[14] A. García-García, A. Vovk, J. A. Pardo, P. Štrichovanec, P. A. Algarabel, C. Magén, J. M. De Teresa, L. Morellón, and M. R. Ibarra, J. Appl. Phys. **107**, 033704 (2010).
[15] A. García-García, J. A. Pardo, P. Štrichovanec, C. Magén, A. Vovk, J. M. De Teresa, G. N. Kakazei, Y. G. Pogorelov, L. Morellón, P. A. Algarabel, and M. R. Ibarra, Appl. Phys. Lett. **98**, 122502 (2011).
[16] H. Raanaei, H. Lidbaum, A. Liebig, K. Leifer, and B. Hjörvarsson, J. Phys.: Condens. Matter **20**, 055212 (2008).
[17] T. Shimada, Y. Ishii, and T. Kitamura, Phys. Rev. B **81**, 134420 (2010).
[18] W. H. Butler, X.-G. Zhang, T. C. Schulthess, and J. M. MacLaren, Phys. Rev. B **63**, 054416 (2001).
[19] J. Mathon and A. Umerski, Phys. Rev. B **63**, 220403 (2001).
[20] G.-X. Miao, M. Münzenberg, and J. S. Moodera, Rep. Prog. Phys. **74**, 036501 (2011).
[21] U. Bauer, M. Przybylski, J. Kirschner, and G. S. D. Beach, Nano Lett. **12**, 1437 (2012).
[22] C. A. F. Vaz, J. Phys.: Condens. Matter **24**, 333201 (2012).
[23] Shufen Zhang, Phys. Rev. Lett. **83**, 640 (1999).
[24] Kohji Nakamura, Toru Akiyama, Tomonori Ito, M. Weinert, and A. J. Freeman, Phys. Rev. B **81**, 220409(R) (2010).

[25]S. M. Jordan, J. F. Lawler, R. Schad, and H. van Kempen, J. Appl. Phys. **84**, 1499 (1998).
[26]K.-H. Kim, H.-J. Kim, J.-P. Ahn, S.-C. Lee, S. O. Won, J. W. Choi, and J. Chang, J. Appl. Phys. **110**, 114910 (2011).
[27]H. L. Meyerheim, R. Popescu, J. Kirschner, N. Jedrecy, M. Sauvage-Simkin, B. Heinrich, and R. Pinchaux, Phys. Rev. Lett. **87**, 076102 (2001).
[28]C. Tusche, H. L. Meyerheim, N. Jedrecy, G. Renaud, A. Ernst, J. Henk, P. Bruno, and J. Kirschner, Phys. Rev. Lett. **95**, 176101 (2005).
[29]X.-G. Zhang, W. H. Butler, and A. Bandyopadhyay, Phys. Rev. B **68**, 092402 (2003).
[30]S. G. Wang, G. Han, G. H. Yu, Y. Jiang, C. Wang, A. Kohn, and R. C. C. Ward, J. Magn. Magn. Mater. **310**, 1935 (2007).
[31]Jinwoo Park and B. D. Yu, Phys. Rev. B **83**, 144431 (2011).
[32]P. Zermatten, F. Bonell, S. Andrieu, M. Chshiev, C. Tiusan, A. Schuhl, and G. Gaudin, Appl. Phys. Express **5**, 023001 (2012).
[33]P. Luches, S. Benedetti, M. Liberati, F. Boscherini, I. I. Pronin, and S. Valeri, Surf. Sci. **583**, 191 (2005).
[34]M. Sicot, S. Andrieu, F. Bertran, and F. Fortuna, Phys. Rev. B **72**, 144414 (2005).
[35]M. Sicot, S. Andrieu, C. Tiusan, F. Montaigne, and F. Bertran, J. Appl. Phys. **99**, 08D301 (2006).
[36]L. Plucinski, Y. Zhao, B. Sinkovic, and E. Vescovo, Phys. Rev. B **75**, 214411 (2007).
[37]S. Colonna, A. Cricenti, P. Luches, S. Valeri, F. Boscherini, J. Qi, Y. Xu, and N. Tolk, Superlattices Microstruct. **46**, 107 (2009).
[38]X. Feng, O. Bengone, M. Alouani, S. Lebègue, I. Rungger, and S. Sanvito, Phys. Rev. B **79**, 174414 (2009).
[39]H. X. Yang, M. Chshiev, A. Kalitsov, A. Schuhl, and W. H. Butler, Appl. Phys. Lett. **96**, 262509 (2010).
[40]S. Hine, T. Shinjo, and T. Takada, J. Phys. Soc. Japan **47**, 767 (1979).
[41]Cs. Fetzer, I. Dézsi, I. Szűcs, F. Tanczikó, and A. G. Balogh, Surf. Sci. **603**, 3021 (2009).
[42]E. Schuster, R. A. Brand, F. Stromberg, F.-Y. Lo, A. Ludwig, D. Reuter, A. D. Wieck, S. Hövel, N. C. Gerhardt, M. R. Hofmann, H. Wende, and W. Keune, J. Appl. Phys. **108**, 063902 (2010).
[43]C. Martínez Boubeta, C. Clavero, J. M. García-Martin, G. Armelles, A. Cebollada, L. Balcells, J. L. Menéndez, F. Peiró, A. Cornet, and M. F. Toney, Phys. Rev. B **71**, 014407 (2005).
[44]S.-H. Yang, B. Balke, C. Papp, S. Döring, U. Berges, L. Plucinski, C. Westphal, C. M. Schneider, S. S. P. Parkin, and C. S. Fadley, Phys. Rev. B **84**, 184410 (2011).
[45]J. I. Beltrán, L. Balcells, and C. Martínez-Boubeta, Phys. Rev. B **85**, 064417 (2012).
[46]J. Korecki, M. Kubik, N. Spiridis, and T. Slezak, Acta Physica Polonica A **97**, 129 (2000).
[47]K. Fukumura, A. Nakanishi, and T. Kobayashi, Nucl. Instrum. Methods Phys. Res. Sect. B **86**, 387 (1994).
[48]M. J. Evans and P. J. Black, J. Phys. C: Solid State Phys. **3**, 2167 (1970).
[49]J. L. Dormann, D. Fiorani, and E. Tronc, Adv. Chem. Phys. **98**, 283 (1997).
[50]J. Hesse and A. Rübartsch, J. Phys. E: Sci. Instrum. **7**, 526 (1974).
[51]H. Keller, J. Appl. Phys. **52**, 5268 (1981).
[52]C. A. McCammon and D. C. Price, Phys. Chem. Miner. **11**, 250 (1985).
[53]C. Wilkinson, A. K. Cheetham, G. J. Long, P. D. Battle, and D. A. O. Hope, Inorg. Chem. **23**, 3136 (1984).
[54]G. A. Waychunas, W. A. Dollase, and C. R. Ross, Am. Mineral. **79**, 274 (1994).
[55]J. Gurgul, E. Młyńczak, N. Spiridis, and J. Korecki, Surf. Sci. **606**, 711 (2012).
[56]G. Lugert and G. Bayreuther, Phys. Rev. B **38**, 11068 (1988).
[57]J. Balogh, D. Kaptás, I. Vincze, K. Temst, and C. Van Haesendonck, Phys. Rev. B **76**, 052408 (2007).
[58]B. R. Cuenya, W. Keune, Dongqi Li, and S. D. Bader, Phys. Rev. B **71**, 064409 (2005).
[59]S. Ohnishi, M. Weinert, and A. J. Freeman, Phys. Rev. B **30**, 36 (1984).
[60]S. Monso, B. Rodmacq, S. Auffret, G. Casali, F. Fettar, B. Gilles, B. Dieny, and P. Boyer, Appl. Phys. Lett. **80**, 4157 (2002).
[61]A. Manchon, C. Ducruet, L. Lombard, S. Auffret, B. Rodmacq, B. Dieny, S. Pizzini, J. Vogel, V. Uhlíř, M. Hochstrasser, and G. Panaccione, J. Appl. Phys. **104**, 043914 (2008).
[62]H. X. Yang, M. Chshiev, B. Dieny, J. H. Lee, A. Manchon, and K. H. Shin, Phys. Rev. B **84**, 054401 (2011).
[63]M. T. Johnson, P. J. H. Bloemen, F. J. A. den Broeder, and J. J. de Vries, Rep. Prog. Phys. **59**, 1409 (1996).
[64]D. Sander, Rep. Prog. Phys. **62**, 809 (1999).
[65]T. Koyano, E. Kita, K. Ohshima, and A. Tasaki, J. Phys.: Condens. Matter **3**, 5921 (1991).
[66]J. Balogh, Cs. Fetzer, D. Kaptás, L. F. Kiss, I. S. Szűcs, I. Dézsi, and I. Vincze, Phys. Status Solidi A **8**, 1828 (2008).